

## Opinion

## Embracing 3D Complexity in Leaf Carbon–Water Exchange

J. Mason Earles,<sup>1,12</sup> Thomas N. Buckley,<sup>2,12</sup> Craig R. Brodersen,<sup>1</sup> Florian A. Busch,<sup>3</sup> F. Javier Cano,<sup>4</sup> Brendan Choat,<sup>4</sup> John R. Evans,<sup>3</sup> Graham D. Farquhar,<sup>3</sup> Richard Harwood,<sup>5</sup> Minh Huynh,<sup>5</sup> Grace P. John,<sup>6</sup> Megan L. Miller,<sup>7</sup> Fulton E. Rockwell,<sup>8</sup> Lawren Sack,<sup>6</sup> Christine Scoffoni,<sup>9</sup> Paul C. Struik,<sup>10</sup> Alex Wu,<sup>11</sup> Xinyou Yin,<sup>10</sup> and Margaret M. Barbour<sup>5,13,\*,@</sup>

**Leaves are a nexus for the exchange of water, carbon, and energy between terrestrial plants and the atmosphere. Research in recent decades has highlighted the critical importance of the underlying biophysical and anatomical determinants of CO<sub>2</sub> and H<sub>2</sub>O transport, but a quantitative understanding of how detailed 3D leaf anatomy mediates within-leaf transport has been hindered by the lack of a consensus framework for analyzing or simulating transport and its spatial and temporal dynamics realistically, and by the difficulty of measuring within-leaf transport at the appropriate scales. We discuss how recent technological advancements now make a spatially explicit 3D leaf analysis possible, through new imaging and modeling tools that will allow us to address long-standing questions related to plant carbon–water exchange.**

### Why Does 3D Matter For Leaf Function?

The leaves of green plants are a striking example of the nexus of structure and function, and of physiology and environment. Here carbon, water, and energy dance through multiple phases, tissues, and scales in a complex 3D landscape that has evolved and diversified under selection for effective exchange in contrasting environments. Yet plant biologists have often resorted to simple leaf-scale models to study these processes – evading the difficult, confounding, and beautiful 3D reality.

It is now well established that CO<sub>2</sub> supply to the sites of photosynthesis (i.e., inside chloroplasts) is limited not only by stomata, but also by a 3D network of resistances within the leaf, collectively termed mesophyll resistance; the pathways for CO<sub>2</sub> diffusion are further complicated by (photo) respiratory CO<sub>2</sub> release in the mitochondria. Yet the precise locations and dynamics of resistances within the mesophyll, their sensitivities to the internal and external environment of the leaf, and their influence on the regulation of net photosynthetic rate remain poorly understood. Similarly, recent research on the 3D architecture of leaf water transport has established the existence of large water potential gradients outside the leaf xylem minor veins. These gradients develop as a result of transport resistances within the leaf, are influenced by temperature and radiation absorption, and may contribute to stomatal dynamics and leaf vulnerability to dehydration.

Imaging and simulation technology can now reproduce the inner reality of the leaf in a **3D image** (see [Glossary](#)) with a clarity and resolution inconceivable a generation ago ([Figure 1](#)). Continued progress in understanding how leaf structure affects function hinges on embracing the structural complexity of real leaves using technologies now widely available ([Table 1](#)). The

### Highlights

Plant biologists have long resorted to highly simplified 1D or 2D imaging methods and modeling to study fundamentally 3D leaf processes of CO<sub>2</sub> and H<sub>2</sub>O transport.

Recent advances in imaging and computational technology are enabling a data-rich scientific pipeline that integrates leaf 3D measurement, anatomical modeling, and biophysical simulation.

Adopting a 3D approach is not only critical for testing when dimensionality reduction is reliable and accurate, but also promises to deliver insights about: (i) fundamental processes of leaf CO<sub>2</sub> and H<sub>2</sub>O transport and exchange, (ii) the translation of leaf anatomical diversity to functional diversity, and (iii) fine-scale CO<sub>2</sub> and H<sub>2</sub>O exchange processes in broader-scale models.

<sup>1</sup>School of Forestry & Environmental Studies, Yale University, New Haven, CT 06511, USA

<sup>2</sup>Department of Plant Sciences, University of California Davis, CA 95916, USA

<sup>3</sup>Research School of Biology, Australian National University, Acton, ACT 0200, Australia

<sup>4</sup>Hawkesbury Institute for the Environment, Western Sydney University, Richmond, NSW 2753, Australia

<sup>5</sup>University of Sydney, Sydney, NSW 2006, Australia

<sup>6</sup>Department of Ecology and Evolutionary Biology, University of California Los Angeles, CA 90095, USA

potential payoffs of a focused and coordinated effort on these problems are great, both for understanding how anatomical diversity translates into functional diversity and for harnessing that knowledge to improve the photosynthetic performance of crops.

### Limitations of a Bulk-Leaf Paradigm for Leaf CO<sub>2</sub> and H<sub>2</sub>O Transport

Photosynthesis, respiration, and transpiration are governed by biochemical and transport processes at several spatial scales within and among multiple tissue types throughout the leaf. Most commonly, however, the leaf has been implicitly treated as a single point with no spatial structure, representing a CO<sub>2</sub> sink during photosynthesis (or source during darkness) and an H<sub>2</sub>O source during transpiration (or sink during dewfall). These point sources and sinks are connected to the atmosphere through resistances arranged in series (e.g., through stomata and the leaf boundary layer), and Fick's first law of diffusion is used to calculate rates of gas exchange with the atmosphere. A biochemical model is used to simulate the photosynthetic CO<sub>2</sub> sink [1], and the H<sub>2</sub>O source is modeled as a wet surface in equilibrium with intercellular air at the measured leaf temperature.

This approach of aggregating transport and biochemistry at the leaf scale has driven tremendous advances by providing a simple bridge between processes at the cell and tissue scales and observations at the leaf scale. However, a bulk-leaf approach precludes understanding how the geometry and biochemistry of different tissue types within the leaf influence CO<sub>2</sub> and H<sub>2</sub>O exchange. The photosynthetic rate of a single chloroplast depends on light intensity, [CO<sub>2</sub>], temperature, and photosynthetic capacity, all of which vary throughout the leaf because of the gradients generated by the interplay of transport with leaf structure. Thus, any single chloroplast is influenced by 3D leaf structure in ways that simple models cannot easily resolve [2,3]. Similarly, complex spatial gradients in metabolites, the allocation of resources such as nitrogen, and temperature and water potential can influence water transport, stomatal function, and metabolism [4–8].

### Spatial Aggregation Conflates Structural Features with Transport Processes

Because leaf CO<sub>2</sub> transport and metabolism are not neatly organized into macroscopic compartments, leaf-scale models and measurements inevitably mask a great deal of structural and process complexity. For example, mesophyll conductance ( $g_m$ ), which describes 3D diffusional pathways between the intercellular airspaces and the chloroplast, is typically computed from bulk-leaf estimates of intercellular CO<sub>2</sub> concentration ( $c_i$ ), chloroplast CO<sub>2</sub> concentration ( $c_c$ ), and leaf net CO<sub>2</sub> assimilation rate ( $A$ ) [9] and traditionally thought to be strongly related to averaged mesophyll anatomy traits including cell wall thickness and chloroplast surface area [10]. **Apparent mesophyll conductance** [11;  $g_{m,app}$ ] is a better term because in real leaves, both  $c_i$  and  $c_c$  vary considerably within a leaf and are dependent on the 3D distribution and biochemical properties of CO<sub>2</sub> sinks and sources [11–16] – features that can vary in ways not consistent with the conceptualization of  $g_m$  as describing fixed pathways. As a result, some effects of environmental conditions on bulk-leaf  $g_{m,app}$  may not reflect shifts in intrinsic transport properties, but may instead result from averaging fluxes and concentrations across the 3D leaf structure or from fine-scale positioning of CO<sub>2</sub> sources relative to sinks.

For example, an effect of irradiance on  $g_{m,app}$  can emerge from changes in the contributions of different mesophyll layers to CO<sub>2</sub> uptake, despite constant transport properties in each layer [17], and chloroplast movement in response to light can alter  $g_{m,app}$  by changing the spatial relationship between supply pathways and reactive demand for CO<sub>2</sub> [18]. Similarly, CO<sub>2</sub> released from mitochondria can be refixed by chloroplasts, which can enhance  $g_{m,app}$  and photosynthesis by providing a CO<sub>2</sub> source close to the photosynthetic sink [19]. Yet, the

<sup>7</sup>College of Natural Resources, University of Idaho, Moscow, ID 83844, USA

<sup>8</sup>Department of Organism and Evolutionary Biology, Harvard University, Cambridge, MA 02138, USA

<sup>9</sup>Department of Biological Sciences, California State University Los Angeles, CA 90032, USA

<sup>10</sup>Department of Plant Sciences, Wageningen University, Centre for Crop Systems Analysis, 6700 AK Wageningen, The Netherlands

<sup>11</sup>Centre for Plant Science, The University of Queensland, Brisbane, QLD 4072, Australia

<sup>12</sup>Equal contribution

<sup>13</sup>[www.sydney.edu.au/science/people/margaret.barbour](http://www.sydney.edu.au/science/people/margaret.barbour)

©Twitter: @Prof\_Margaret

\*Correspondence: [margaret.barbour@sydney.edu.au](mailto:margaret.barbour@sydney.edu.au) (M.M. Barbour).

likelihood of refixation depends on the relative positions of mitochondria and chloroplasts, which can shift over time [20,21]. Clearly these patterns and dynamics need to be accounted for in future models seeking to predict  $g_{m,app}$  at the leaf scale.

Similar issues arise in relation to functional traits other than  $g_m$ . For example, a mismatch between light absorption and photosynthetic capacity among mesophyll layers can affect the response of CO<sub>2</sub> uptake to irradiance and light quality [22–24] and hinder the interpretation of chlorophyll fluorescence [25]. Although transdermally explicit models of photosynthesis have been used to address these questions [26,27], the role of leaf anatomical diversity remains largely unexplored. In addition, the distribution of enzymes and metabolites influences metabolic fluxes measured at the leaf level [28]. A full understanding of photosynthetic function in intact leaves thus requires high resolution and/or spatially explicit treatments of CO<sub>2</sub> transport to understand estimates of  $g_m$  using both the stable isotope and the fluorescence methods [2].

### Aggregating to the Tissue Scale Limits Understanding

Some important parameters that affect water transport in leaves remain poorly known, because they depend on fine-scale features that cannot be accurately measured with traditional imaging or experimental methods, and this hinders attempts to model water transport [6,7,29–31]. One example is tangential water flow through cell walls outside the xylem, which depends on anatomical features that are difficult to discern in 2D light micrographs, such as cell wall thickness and the location and extent of hydrophobic barriers to water flow such as lignin or suberin, and forms a major component of **leaf hydraulic conductance**. The lateral connectivity or contact area between cells also affects transport but is difficult to estimate accurately from 2D light micrographs, particularly for cells with highly variable shapes within the vascular parenchyma, bundle sheath, and mesophyll. Our ability to model water movement within the leaf xylem may also be improved by 3D approaches that capture the arrangement and connections between xylem conduits. The complexity of water movement through the xylem is increased as some conduits in the leaf vein network become gas filled (embolized) due to water stress [32].

Another process which depends on 3D tissue arrangement is water vapor transport, which is typically modeled by assuming the air is in chemical and thermal equilibrium with the nearest liquid water surface, generally a cell wall. This assumption implies that vapor concentration adjacent to the cell surface equals equilibrium vapor pressure of that surface, which can be calculated from its water potential and temperature [6,30,31]. However, because this ‘local equilibrium’ approximation neglects the vapor gradients that must exist across air-filled pore spaces between cells, it will tend to underestimate the total resistance to vapor transport within the leaf, especially as intercellular airspaces become large relative to cell size. Precise quantification of multidirectional vapor transport at these scales requires equally precise resolution of the actual tissue geometries. Indeed, interpretation of recent experiments using 0D models of gas exchange and isotopic enrichment has recently challenged the assumption [33] that the airspaces on the interior side of a stomatal pore are saturated with water vapor at the leaf surface temperature, a dogma that is generally used to define stomatal conductance in gas exchange systems. Fully 3D models of both processes, together with spatially resolved knowledge of cell wall material properties, could play a decisive role in resolving this controversy.

### Reducing Dimensionality Can Generate Bias

It is common to simplify descriptions of leaf anatomy to facilitate modeling and analysis. This simplification discards potentially important data, limiting insights and generating bias.

### Glossary

**3D image:** typically represented as a ‘stack’ of many 2D images, the basic spatial unit of a 3D image is a volumetric pixel, or ‘voxel’. Each voxel in a 3D image is populated with a value that corresponds with the instrument and sensor type. For example, X-ray microCT images contain voxels that quantify the X-ray in a given region which often corresponds with differences in material type, such as water, air, and cell wall.

#### Apparent mesophyll

**conductance:** apparent mesophyll conductance ( $g_m$ ) simplifies the complexity of fluxes and resistances within the mesophyll to an apparent analogy with Fick’s first law of diffusion where the conductance is characterized as the net flux of CO<sub>2</sub> molecules divided by the driven force for diffusion of CO<sub>2</sub> between intercellular airspace and RuBisCO sites inside chloroplasts. It is typically computed from bulk-leaf estimates of internal CO<sub>2</sub> concentration ( $c_i$ ), chloroplastic CO<sub>2</sub> concentration ( $c_c$ ) and measured net CO<sub>2</sub> exchange ( $A$ ), both of which critically depend on the 3D distribution and biochemical properties of CO<sub>2</sub> sinks and sources along the CO<sub>2</sub>-diffusion path.

#### Image segmentation and

**classification:** image segmentation and classification is the process of digitally assigning values to each voxel based on their discrete class. For example, voxels belonging to the intercellular airspace, cells, and veins classes would each be assigned a unique value.

#### Leaf hydraulic conductance:

defined as the ratio of flow rate to the gradient in water potential that drives the flow; leaf hydraulic conductance defines the efficiency with which H<sub>2</sub>O molecules are transported through the inside- and outside-xylem pathways.

**Volumetric mesh:** a volumetric mesh is derived from the raw 3D image and is a common data format used for biophysical simulations. It approximates each segmented class using 3D volumetric elements, such as tetrahedra, blocks, or hexahedra.

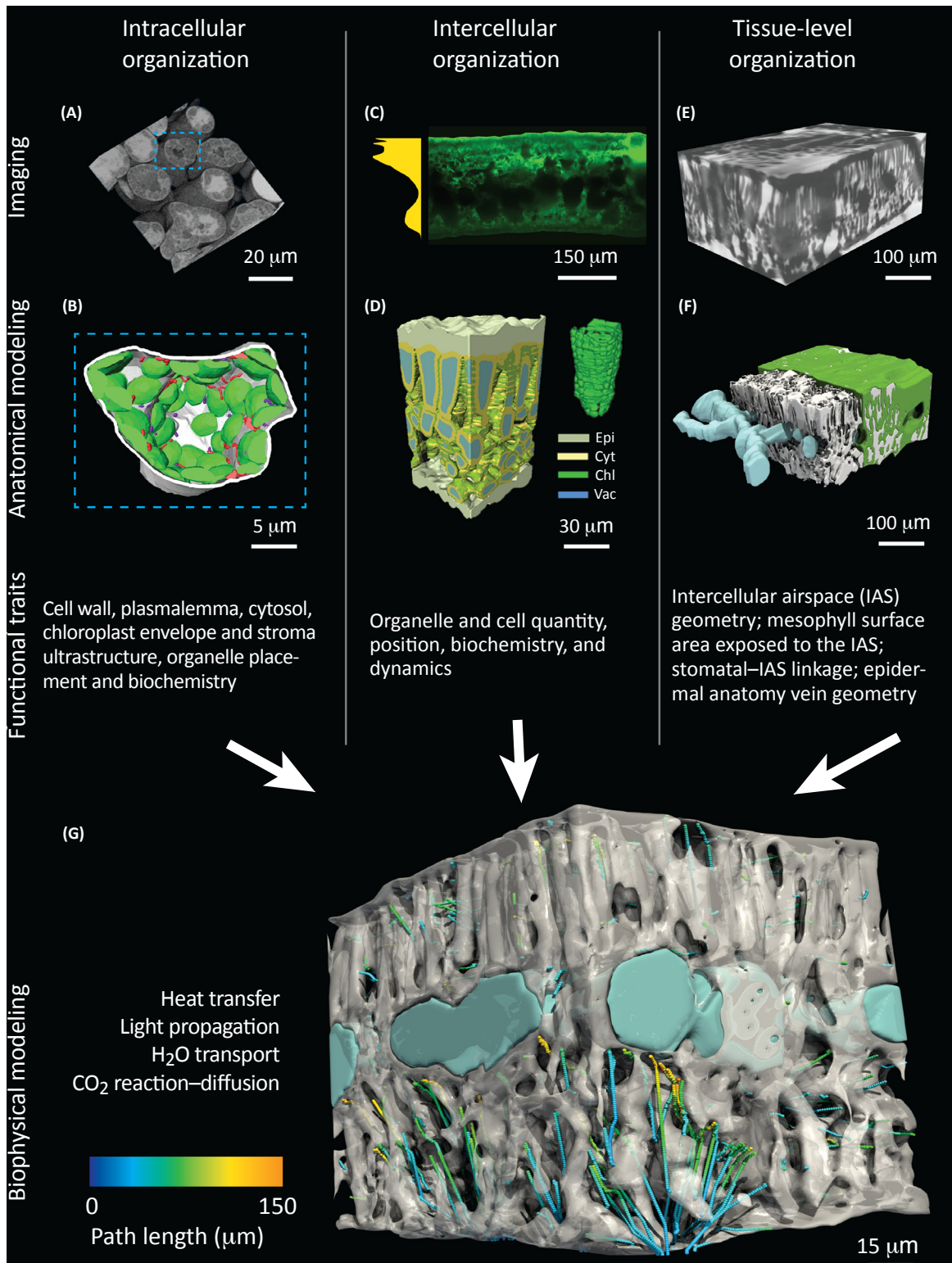


Table 1. Advanced 3D Technologies for Imaging Leaves

	Confocal/MP/LS microscopy <sup>a</sup>	X-ray CT <sup>a</sup>	SBF-SEM <sup>a</sup>	FIB-SEM <sup>a</sup>	TEM tomography
Example Ref	[73]	[74]	[75]	[63]	[62]
Sample preparation	Live or fixed, fluorophore labeling	Live or fixed, heavy-metal stain, whole mount	Fixed, heavy-metal stain, resin embed	Fixed, heavy-metal stain, resin embed	Fixed, heavy-metal stain, resin embed
Sample preparation time	0–2 days	0–2 days	7–14 days	3–5 days	3–5 days
Lateral resolution	200–300 nm	1–40 $\mu\text{m}$ ( $\mu\text{CT}$ )	5–10 nm	2 nm	1 nm
Axial resolution	500 nm	1–40 $\mu\text{m}$ ( $\mu\text{CT}$ )	30–50 nm	3–5 nm	2–3 nm
Field of view	160 $\mu\text{m}$ to 4 mm	1–40 mm	50–300 $\mu\text{m}$	10–100 $\mu\text{m}$	0.5–10 $\mu\text{m}$
Sample size	1 $\times$ 1 mm	up to 50 $\times$ 50 mm	1 $\times$ 1 mm	10 $\times$ 10 mm	up to 200 $\times$ 200 nm
Sample thickness	~300 $\mu\text{m}$	1–50 mm ( $\mu\text{CT}$ )	600 $\mu\text{m}$	10 mm	<200 nm
Imaging time	1–8 h	Minutes to days	1–5 days	1–10 h	1–4 h
Data set size	1–100 MB	5–50 GB	50–500 GB	~100 MB	~1 GB
Visible leaf structure	Mitochondria, chloroplasts, airspace network, cell, cell network, leaf	Cell, cell network, airspace network, leaf	Plasmodesmata, cell membranes, cell wall, mitochondria, chloroplasts	Plasmodesmata, cell membranes, cell wall, mitochondria, chloroplasts	Plasmodesmata, cell membranes, cell wall, mitochondria, chloroplasts

<sup>a</sup>Abbreviations: confocal/MP/LS microscopy, confocal, multiphoton, and/or light sheet microscopy; FIB-SEM, focused ion beam scanning electron microscopy; SBF-SEM, serial block face scanning electron microscopy; TEM, transmission electron microscopy; X-ray CT, X-ray computed tomography.

Mesophyll conductance is again an illustrative example.  $g_m$  includes resistances across intercellular airspaces [2], cell walls [34,35], cell and chloroplast membranes [36–38], and chloroplast stroma [34], and experimental measurements of  $g_m$  integrate across all of these elements. Although isotopic methods can help distinguish the components of  $g_m$  [39,40], there are no experimental methods to directly quantify their spatial variation, which must instead be inferred by applying anatomical measurements to spatially explicit models [25]. Such measurements are commonly simplified to bulk-leaf descriptors – for example, the 3D geometry of leaf intercellular airspaces is often summarized in a single scalar, the porosity (volumetric air fraction), which cannot describe how the multitude of 3D cell shapes and tissue geometries [41,42] impact path length, lateral diffusivity, tortuosity, and airspace connectivity [2,43], nor how the spatial distribution of stomata and mesophyll surfaces influences  $\text{CO}_2$  diffusion into chloroplasts [20]. The surface areas of mesophyll cells and chloroplasts exposed to airspaces also influence  $g_m$  [44] and vary considerably [45], but are commonly estimated from 2D sections

**Figure 1. The 3D Leaf Scientific Pipeline.** Examples of how imaging data can be used to build 3D anatomical leaf models at multiple levels of biological organization: intracellular, intercellular, and tissue level. (A) 3D volumetric image from serial block face scanning electron microscopy of *Triticum aestivum* leaf mesophyll cells (R. Harwood *et al.*, unpublished) used for **image segmentation and classification** to create a **volumetric mesh**. Blue dashed box corresponds to a 3D anatomical model (B) of a partial mesophyll cell that spatially maps the cell wall in white, chloroplasts in green, mitochondria in red, and peroxisomes in purple. (C) 2D image showing chlorophyll absorption profile (gold polygon) in *Ilex opaca* using optical fluorescence microscopy (J.M. Earles *et al.*, unpublished). (D) 3D model of chlorophyll distribution for a *Solanum lycopersicum* leaf from Ho *et al.* [3]; Epi, Cyt, Chl, and Vac indicate epidermal cells, the mesophyll cytosol, chloroplasts, and mesophyll vacuoles, respectively. (E) 3D volumetric image from X-ray micro-computed tomography (microCT) of *Helianthus annuus* leaf where dark and light regions correspond to high and low X-ray absorption, respectively (J.M. Earles *et al.*, unpublished). (F) 3D model of cells in green, intercellular airspace in white, and veins in blue generated from the microCT image in (E); J.M.; Earles *et al.*, unpublished). Key functional traits related to  $\text{CO}_2$  and  $\text{H}_2\text{O}$  transport that can be identified and modeled are discussed for each level of biological organization. Ultimately, parameterizing 3D anatomical models with key functional traits will allow for dynamic modeling of biophysical processes, such as heat transfer, light propagation,  $\text{H}_2\text{O}$  transport, and  $\text{CO}_2$  reaction–diffusion. (G) The partly transparent mesophyll tissue (white) and veins of *H. annuus* with streamlines representing the average  $\text{CO}_2$  diffusive pathways for  $\text{CO}_2$  from stomata throughout the intercellular airspace. Colors represent the geodesic diffusive path length from the nearest stomata to various points along a given diffusive streamline (J.M. Earles *et al.*, unpublished; also see [60] for examples in the Bromeliaceae family).

(Figure legend continued on the bottom of the next page.)

based on simple models for cell shape. Complex cell geometries can confound such estimates and complicate allometric scaling among cell dimensions [17,46].

#### Stable Isotope Discrimination May Depend on 3D Leaf Anatomy

Understanding how bulk-leaf stable isotope discrimination arises from diffusion and exchange at smaller scales would also benefit from a high-resolution, spatially explicit approach. Stable isotopes are important tools for plant physiologists as tracers of atoms through systems that record processes such as carboxylation, mesophyll conductance, and transpiration [47]. Theoretical models describing the underlying biophysics and biochemistry exist, but the most widely applied are spatially aggregated at the leaf level [48]. Examples of attempts to improve on this include adding a conceptual dimension by analyzing CO<sub>2</sub> fluxes in and out of the leaf in parallel [19], adding a spatial dimension by exploring radial isotope effects in leaf water [49–52], or adding a temporal dimension by probing nonsteady state leaf water isotope enrichment [53]. However, there remains no spatially resolved and anatomically accurate 3D model of stable isotope fractionation [54], so we have no means to quantify the influence of 3D anatomy on isotope processes. 3D transport of <sup>13</sup>CO<sub>2</sub> within leaves is of particular interest because one of the primary techniques to estimate  $g_m$  requires a thorough understanding of carbon isotope discrimination within photosynthesizing leaves, and isotopic discrimination (during carboxylation, respiration, photorespiration, retrodiffusion, and refixation) would be influenced by the 3D structure of leaf airspaces, which governs the relationship between diffusion paths and exchanging surfaces, and hence the relative rates of gross and net exchange to and from those surfaces. Similar issues are inherent in interpretation of photosynthetic C<sup>18</sup>O<sup>16</sup>O discrimination [40] and leaf water isotopes [54].

#### Toward a High-Resolution, Spatially Explicit Approach

Applied models of plant-atmosphere CO<sub>2</sub> and H<sub>2</sub>O exchange do not typically represent the leaf interior in a spatially explicit way, because it is impractical with current technology to parameterize and apply microscale spatially explicit models to address questions that integrate over large scales. This practical constraint should inform basic research that takes place within a spatially explicit paradigm (Box 1). In basic research, however, a mechanistically accurate understanding of leaf carbon and water exchange requires that we move beyond the spatially aggregated ‘bulk-leaf’ paradigm in imaging and modeling. Such a high-resolution 3D approach will improve the reliability of leaf-scale models, thus informing their application at larger scales.

An obvious first step is to adopt spatially explicit models in research. Many insights have been generated using such models, with simplified cell, organelle, and tissue geometries, often

##### Box 1. Scaling to the Leaf and Canopy Level

Reliable prediction of global plant-atmosphere interactions [65] and crop yield [66] inevitably involves interaction of modeling efforts at different scales [67]. Complex, mechanistic models must ultimately be simplified for application at larger scales, and likewise, understanding gained from a 3D anatomically explicit paradigm for modeling leaf processes must eventually be shaped into a form that can be applied practically in the context of lower-dimensional or scaled models. Similar considerations have helped the application of leaf-level photosynthesis models to the crop canopy level as a useful tool for estimating consequences of photosynthetic perturbations at the biochemical level [22,68]. Analogously, upscaling of physiological processes that have been improved by 3D analyses and subsequently simplified for the desired purpose will benefit our understanding of their effects on the canopy scale. This perspective should inform research design: for example, in studies using fine-scale 3D-driven imaging and modeling, hypotheses should be framed in terms of anatomical parameters that can be linked to commonly measured leaf traits (e.g., leaf mass per unit area, leaf airspace fraction, or apparent mesophyll conductance). This ensures an immediate conduit for extension of new knowledge from the 3D paradigm to the vast body of existing leaf trait data [69]. Of particular benefit are analyses focused explicitly on anatomical scaling [70,71] and on strategies for mapping 3D transport processes to widely useful 1D models [72] or inferring 3D properties from 1D or 2D imaging data (e.g., tortuosity and porosity).

reconstructed from 2D cross-sectional images, to simulate light propagation [55], CO<sub>2</sub> reaction-diffusion [3, 13, 56–58], and leaf water and energy transport [6, 30, 31]. However, these approaches have typically depended on simplifications of anatomy that may affect model predictions. Thus, a critical and more challenging step is to directly generate 3D tissue models from imaging data, thereby circumventing the abstractions and loss of spatial resolution inherent in simplified models.

Recent advances in microscopy have streamlined the acquisition of 3D volumes at high resolution (e.g., serial block face scanning electron microscopy and focused ion beam scanning electron microscopy; Table 1), and modern computational tools are available for spatially explicit modeling of matter and energy transport (Table 2). Advanced imaging and computation can now quantify tissue geometry directly, alleviating the tedium of extracting measurements by hand from 2D micrographs and the uncertainty created by using assumptions about 3D geometry to infer tissue properties from 2D images. Such studies have indicated that 2D estimates of mesophyll surface area exposed to airspace can be 15–30% lower than 3D measures [59], and inclusion of 3D measurements of airspace tortuosity and lateral path lengthening reduced estimates of diffusional conductance within the intercellular airspace of bromeliad leaves by 37%, on average [60]. Visually segmenting and measuring distinct tissue types and cellular properties require measuring these traits at multiple scales with different microscopy methods (Table 1). Each method presents unique challenges, especially regarding specimen viability, but their spatial and temporal resolution have already delivered novel insight into the effects of 3D tissue and organelle arrangement on photosynthesis [61], viral transmission [62], and salinity stress [63].

Table 2. 3D Biophysical Leaf CO<sub>2</sub> and H<sub>2</sub>O Transport

Biophysical phenomena	Biophysical and computational model	Biophysical traits	Traits measured/inferred at the bulk-leaf level
Heat transfer	3D temperature distribution; depends on radiative, conductive, convective, and latent energy transfer and external and internal energy sources; interacts with light propagation; solved via heat transfer partial differential equations on geometric mesh or finite-element analysis	3D cellular and intercellular airspace network geometry, photosystem light absorption and heat dissipation, H <sub>2</sub> O liquid-vapor transport patterns and interactions	Leaf temperature, leaf hydraulic conductance, apparent mesophyll conductance, respiration, photosynthesis
Light propagation	3D distribution of light intensity and spectral/directional quality; depends on internal absorption and scattering, and external light sources; solved via Monte Carlo ray tracing photon simulation on geometric mesh	Spatiotemporal distribution and geometry of organelles, cells, and tissues/airspace; optical properties of organelle, cell, and tissue material types with respect to light intensity and spectral/directional quality	Apparent mesophyll conductance; respiration; photosynthesis; reflectance, absorptance, and transmittance; chlorophyll fluorescence
H <sub>2</sub> O transport	3D distribution of water potential; depends on bulk flow, diffusion, and evaporation; interacts with heat transfer; solved via mass transport partial differential equations on geometric mesh or infinite-element analysis	3D cellular and intercellular airspace network geometry, aquaporin activity, temperature distribution, leaf liquid water transport conductance inside and outside xylem, leaf water vapor transport, stomatal function	Leaf water potential, transpiration rate, leaf hydraulic conductance, stomatal conductance
CO <sub>2</sub> and metabolite reaction-diffusion	3D distribution of [CO <sub>2</sub> ]; depends on reactive photosynthetic demand, (photo)respiratory supply, and diffusion; interacts strongly with heat transfer and light propagation and weakly with H <sub>2</sub> O vapor diffusion	Spatiotemporal distribution and geometry of organelles, cells, and tissues/airspace; 3D cellular and intercellular airspace network geometry; liquid phase diffusivities; metabolic network structure and flux	Apparent mesophyll conductance, respiration, photosynthesis, intercellular and chloroplastic [CO <sub>2</sub> ], metabolite concentrations

A recent study provides a landmark example of integrated, anatomically explicit 3D modeling of leaf transport [3]. That study applied 3D leaf microstructure data [based on micro-computed tomography (microCT) imaging; Table 1] to modules that calculated light and CO<sub>2</sub> and HCO<sub>3</sub><sup>-</sup> exchange in intercellular airspaces and within cells, with different scenarios for 3D distribution of photosynthetic capacity. This fusion of 3D imaging and modeling technologies enabled several critical insights about refixation of CO<sub>2</sub>, the role of carbonic anhydrase, and the economy of photosynthetic capacity distribution, especially when predictions from the 3D-explicit approach differed systematically from an earlier 2D model [64]. For example, the more realistic representation of the 3D interconnectivity within the intercellular airspaces resulted in 61.7% of (photo)respired CO<sub>2</sub> estimated to be refixed by RuBisCO. An analogous 3D explicit model could provide a more exact description of vapor transport through the intercellular airspaces. Notably, 3D imaging at current resolution will not be sufficient, as some features of transport, such as liquid phase water transport through cell walls and membranes, depend on structural details and material properties that must be determined empirically [6] or built up from nanoscale models of wall, membrane, and cell structure [29].

It is likely that a 3D paradigm will substantially alter our understanding of many of the nuanced questions associated with leaf anatomy and function. Currently, it is unclear *a priori* whether 3D analysis for any given process would lead to qualitatively different understanding. However, the technological advances outlined here are rapidly obviating any justification for adhering to the status quo (i.e., the spatially aggregated approach to studying leaf transport) without first, or concurrently, evaluating the results of analyses informed by high-resolution, spatially explicit approaches. A reasonable goal that could be achieved within the next decade with a coordinated, collaborative approach is to characterize internal leaf anatomy in detail for a few model species representing a range of plant functional types, and to apply the resulting data to a 3D model of leaf transport. Comparing predictions to leaf-scale gas exchange measurements would help determine how diversity of leaf structure affects photosynthesis and transpiration, and how to account for these effects in traditional leaf-scale models. Thus, the leaf biology communities should embrace a 3D approach with all its complexity, and all its promise (see also Outstanding Questions).

### Acknowledgments

This work was supported by the University of Sydney through the SREI 2020 scheme and by the ARC Centre for Translational Photosynthesis. M.M.B. and R.H. acknowledge the facilities of the Australian Microscopy and Microanalysis Research Facility at Sydney Microscopy and Microanalysis, and technical assistance from Timur Burykin and Elinor Goodman.

### References

1. Farquhar, G.D. *et al.* (1980) A biochemical model of photosynthetic CO<sub>2</sub> assimilation in leaves of C<sub>3</sub> species. *Planta* 149, 78–90
2. Parkhurst, D.F. (1994) Tansley review no. 65. Diffusion of CO<sub>2</sub> and other gases inside leaves. *New Phytol.* 126, 449–479
3. Ho, Q.T. *et al.* (2016) Three-dimensional microscale modelling of CO<sub>2</sub> transport and light propagation in tomato leaves enlightens photosynthesis. *Plant Cell Environ.* 39, 50–61
4. Pieruschka, R. *et al.* (2010) The control of transpiration by absorbed radiation. *Proc. Natl. Acad. Sci. U. S. A.* 107, 13372–13377
5. Mott, K.A. and Peak, D. (2011) Alternative perspective on the control of transpiration by radiation. *Proc. Natl. Acad. Sci. U. S. A.* 108, 19820–19823
6. Rockwell, F.E. *et al.* (2014) The competition between liquid and vapor transport in transpiring leaves. *Plant Physiol.* 164, 1741–1758
7. Rockwell, F.E. *et al.* (2014) Leaf hydraulics I: scaling transport properties from single cells to tissues. *J. Theor. Biol.* 340, 251–266
8. Wang, S. *et al.* (2017) C<sub>4</sub> photosynthesis in C<sub>3</sub> rice: a theoretical analysis of biochemical and anatomical factors. *Plant Cell Environ.* 40, 80–94
9. Flexas, J. *et al.* (2008) Mesophyll conductance to CO<sub>2</sub>: current knowledge and future prospects. *Plant Cell Environ.* 31, 602–621
10. Evans, J.R. *et al.* (1994) The relationship between CO<sub>2</sub> transfer conductance and leaf anatomy in transgenic tobacco with a reduced content of Rubisco. *Aust. J. Plant Physiol.* 21, 475–495
11. Tholen, D. *et al.* (2012) Variable mesophyll conductance revisited: theoretical background and experimental implications. *Plant Cell Environ.* 35, 2087–2103
12. Terashima, I. and Inoue, Y. (1984) Comparative photosynthetic properties of palisade tissue chloroplasts and spongy tissue chloroplasts of *Camellia japonica* L.: functional adjustment of the photosynthetic apparatus to light environment within a leaf. *Plant Cell Physiol.* 25, 555–563
13. Tholen, D. and Zhu, X.-G. (2011) The mechanistic basis of internal conductance: a theoretical analysis of mesophyll cell photosynthesis and CO<sub>2</sub> diffusion. *Plant Physiol.* 156, 90–105

### Outstanding Questions

#### Light propagation and absorption:

How does the 3D anatomical, biochemical, and biophysical arrangement of organelles, cells, airspace, and tissue types influence light propagation, absorption, and ultimately CO<sub>2</sub> and H<sub>2</sub>O transport?

#### Interorganellar CO<sub>2</sub> exchange:

How does the spatial arrangement of organelles, such as chloroplasts, mitochondria, and vacuoles, influence CO<sub>2</sub> transport through the liquid phase of the cell? What is the resulting effect on CO<sub>2</sub> fixation, release, and refixation associated with photosynthesis and respiration? To which degree do plants modify these anatomical properties, and do these modifications convey a carbon benefit in given environments?

#### H<sub>2</sub>O transport pathways:

What is the influence of the 3D anatomical arrangement of membrane transporters, organelles, cells, airspace, and tissue types on water potential gradients within the leaf? What is the resulting effect on stomatal dynamics and transpiration?

#### Spatial coordination of intraleaf CO<sub>2</sub> and H<sub>2</sub>O sources and sinks:

How does the geometric arrangement of stomata, organelles, and intercellular airspaces influence light absorption and affect leaf internal CO<sub>2</sub> concentration gradients within leaves? What are the resulting effects on photosynthetic rate at the whole leaf level? To what extent does internal leaf geometry modulate water use efficiency of leaves? What are the evolutionary and adaptive solutions of plants to deal with environmental heterogeneity?

#### Isotope discrimination:

How does leaf internal 3D anatomical arrangement affect stable isotope fractionation and what are the implications of these effects for estimates of mesophyll conductance?

14. Hogewoning, S.W. *et al.* (2012) Photosynthetic quantum yield dynamics: from photosystems to leaves. *Plant Cell* 24, 1921–1935
15. Tcherkez, G. *et al.* (2012) Respiratory carbon fluxes in leaves. *Curr. Opin. Plant Biol.* 15, 308–314
16. Tcherkez, G. (2013) Is the recovery of (photo) respiratory CO<sub>2</sub> and intermediates minimal? *New Phytol.* 198, 334–338
17. Thérroux-Rancourt, G. and Gilbert, M.E. (2017) The light response of mesophyll conductance is controlled by structure across leaf profiles. *Plant Cell Environ.* 40, 726–740
18. Tholen, D. *et al.* (2008) The chloroplast avoidance response decreases internal conductance to CO<sub>2</sub> diffusion in *Arabidopsis thaliana* leaves. *Plant Cell Environ.* 31, 1688–1700
19. Busch, F.A. *et al.* (2013) C<sub>3</sub> plants enhance rates of photosynthesis by reassimilating photorespired and respired CO<sub>2</sub>. *Plant Cell Environ.* 36, 200–212
20. Berghuijs, H.N.C. *et al.* (2016) Mesophyll conductance and reaction-diffusion models for CO<sub>2</sub> transport in C<sub>3</sub> leaves: needs, opportunities and challenges. *Plant Sci.* 252, 62–75
21. Yin, X. and Struik, P.C. (2017) Can increased leaf photosynthesis be converted into higher crop mass production? A simulation study for rice using the crop model GECROS. *J. Exp. Bot.* 68, 2345–2360
22. Ögren, E. and Evans, J.R. (1993) Photosynthetic light response curves. 1. The influence of CO<sub>2</sub> partial pressure and leaf inversion. *Planta* 189, 182–190
23. Vogelmann, T.C. and Evans, J.R. (2002) Profiles of light absorption and chlorophyll within spinach leaves from chlorophyll fluorescence. *Plant Cell Environ.* 25, 1313–1323
24. Earles, J.M. *et al.* (2017) Excess diffuse light absorption in upper mesophyll limits CO<sub>2</sub> drawdown and depresses photosynthesis. *Plant Physiol.* 174, 1082–1096
25. Evans, J.R. *et al.* (2017) Light quality affects chloroplast electron transport rates estimated from chl fluorescence measurements. *Plant Cell Physiol.* 58, 1652–1660
26. Hikosaka, K. and Terashima, I. (1995) A model of the acclimation of photosynthesis in the leaves of C<sub>3</sub> plants to sun and shade with respect to nitrogen use. *Plant Cell Environ.* 18, 605–618
27. Buckley, T.N. and Farquhar, G.D. (2004) A new analytical model for whole-leaf potential electron transport rate. *Plant Cell Environ.* 27, 1487–1502
28. Mintz-Oron, S. *et al.* (2012) Reconstruction of *Arabidopsis* metabolic network models accounting for subcellular compartmentalization and tissue-specificity. *Proc. Natl. Acad. Sci. U. S. A.* 109, 339–344
29. Buckley, T.N. (2015) The contributions of apoplastic, symplastic and gas phase pathways for water transport outside the bundle sheath in leaves. *Plant Cell Environ.* 38, 7–22
30. Buckley, T.N. *et al.* (2015) How does leaf anatomy influence water transport outside the xylem? *Plant Physiol.* 168, 1616–1635
31. Buckley, T.N. *et al.* (2017) The sites of evaporation within leaves. *Plant Physiol.* 173, 1763–1782
32. Choat, B. *et al.* (2018) Triggers of tree mortality under drought. *Nature* 558, 531–539
33. Cernusak, L.A. *et al.* (2018) Unsaturation of vapour pressure inside leaves of two conifer species. *Sci. Rep.* 8, 7667
34. Evans, J.R. *et al.* (2009) Resistances along the CO<sub>2</sub> diffusion pathway inside leaves. *J. Exp. Bot.* 60, 2235–2248
35. Veromann-Jürgenson, L.L. *et al.* (2017) Extremely thick cell walls and low mesophyll conductance: welcome to the world of ancient living! *J. Exp. Bot.* 68, 1639–1653
36. Hanba, Y.T. *et al.* (2004) Overexpression of the barley aquaporin HvPIP2;1 increases internal CO<sub>2</sub> conductance and CO<sub>2</sub> assimilation in the leaves of transgenic rice plants. *Plant Cell Physiol.* 45, 521–529
37. Flexas, J. *et al.* (2006) Tobacco aquaporin NtAQP1 is involved in mesophyll conductance to CO<sub>2</sub> *in vivo*. *Plant J.* 48, 427–439
38. Groszmann, M. *et al.* (2017) Carbon dioxide and water transport through plant aquaporins. *Plant Cell Environ.* 40, 938–961
39. Gillon, J.S. and Yakir, D. (2000) Internal conductance to CO<sub>2</sub> diffusion and C<sup>18</sup>O discrimination in C<sub>3</sub> leaves. *Plant Physiol.* 123, 201–214
40. Barbour, M.M. *et al.* (2016) Online CO<sub>2</sub> and H<sub>2</sub>O oxygen isotope fractionation allows estimation of mesophyll conductance in C<sub>4</sub> plants, and reveals that mesophyll conductance decreases as leaves age in both C<sub>4</sub> and C<sub>3</sub> plants. *New Phytol.* 210, 875–889
41. Terashima, I. *et al.* (2011) Leaf functional anatomy in relation to photosynthesis. *Plant Physiol.* 155, 108–116
42. Tosens, T. *et al.* (2012) Anatomical basis of variation in mesophyll resistance in eastern Australian sclerophylls: news of a long and winding path. *J. Exp. Bot.* 63, 5105–5119
43. Pieruschka, R. *et al.* (2005) Lateral gas diffusion inside leaves. *J. Exp. Bot.* 56, 857–864
44. Tosens, T. *et al.* (2012) Developmental changes in mesophyll diffusion conductance and photosynthetic capacity under different light and water availabilities in *Populus tremula*: how structure constrains function. *Plant Cell Environ.* 35, 839–856
45. Onoda, Y. *et al.* (2017) Physiological and structural tradeoffs underlying the leaf economics spectrum. *New Phytol.* 214, 1447–1463
46. Sage, T.L. and Sage, R.F. (2009) The functional anatomy of rice leaves: implications for refixation of photorespiratory CO<sub>2</sub> and efforts to engineer C<sub>4</sub> photosynthesis into rice. *Plant Cell Physiol.* 50, 756–772
47. Yakir, D. and Sternberg, L.S.L. (2000) The use of stable isotopes to study ecosystem gas exchange. *Oecologia* 123, 297–311
48. Farquhar, G.D. and Richards, R.A. (1984) Isotopic composition of plant carbon correlates with water-use efficiency of wheat genotypes. *Aust. J. Plant Physiol.* 11, 539–552
49. Gan, K.S. *et al.* (2002) <sup>18</sup>O spatial patterns of vein xylem water, leaf water, and dry matter in cotton leaves. *Plant Physiol.* 130, 1008–1021
50. Gan, K.S. *et al.* (2003) Evaluation of models of leaf water <sup>18</sup>O enrichment using measurements of spatial patterns of vein xylem water, leaf water and dry matter in maize leaves. *Plant Cell Environ.* 26, 1479–1495
51. Ogée, J. *et al.* (2007) Non-steady-state, non-uniform transpiration rate and leaf anatomy effects on the progressive stable isotope enrichment of leaf water along monocot leaves. *Plant Cell Environ.* 30, 367–387
52. Gerlein-Safdi, C. *et al.* (2017) Leaf water <sup>18</sup>O and <sup>2</sup>H maps show directional enrichment discrepancy in *Colocasia esculenta*. *Plant Cell Environ.* 40, 2095–2108
53. Farquhar, G.D. and Cernusak, L.A. (2005) On the isotopic composition of leaf water in the non-steady state. *Funct. Plant Biol.* 32, 293–303
54. Barbour, M.M. *et al.* (2017) Leaf water stable isotopes and water transport outside the xylem. *Plant Cell Environ.* 40, 914–920
55. Xiao, Y. *et al.* (2016) The influence of leaf anatomy on the internal light environment and photosynthetic electron transport rate: exploration with a new leaf ray tracing model. *J. Exp. Bot.* 67, 6021–6035
56. Parkhurst, D.F. (1977) A three-dimensional model for CO<sub>2</sub> uptake by continuously distributed mesophyll in leaves. *J. Theor. Biol.* 67, 471–488
57. Vesala, T. *et al.* (1996) Analysis of stomatal CO<sub>2</sub> uptake by a three-dimensional cylindrically symmetric model. *New Phytol.* 132, 235–245
58. Aalto, T. and Juurola, E. (2002) A three-dimensional model of CO<sub>2</sub> transport in airspaces and mesophyll cells of a silver birch leaf. *Plant Cell Environ.* 25, 1399–1409
59. Thérroux-Rancourt, G. *et al.* (2017) The bias of a two-dimensional view: comparing two-dimensional and three-dimensional mesophyll surface area estimates using noninvasive imaging. *New Phytol.* 215, 1609–1622
60. Earles, J.M. *et al.* (2018) Beyond porosity: 3D leaf intercellular airspace traits than impact mesophyll conductance. *Plant Physiol.* Published online July 24, 2018. <http://dx.doi.org/10.1104/pp.18.00550>

61. Lehmeier, C. *et al.* (2017) Cell density and airspace patterning in the leaf can be manipulated to increase leaf photosynthetic capacity. *Plant J.* 92, 981–994
62. Jin, X. *et al.* (2017) Three-dimensional analysis of chloroplast structures associated with virus infection. *Plant Physiol.* 176, 282–294
63. Yamane, K. *et al.* (2017) Three-dimensional ultrastructure of chloroplast pockets formed under salinity stress. *Plant Cell Environ.* 41, 563–575
64. Ho, Q.T. *et al.* (2012) A microscale model for combined CO<sub>2</sub> diffusion and photosynthesis in leaves. *PLoS One* 7, e48376
65. Faticchi, S. *et al.* (2016) Modeling plant-water interactions: an ecohydrological overview from the cell to the global scale. *WIREs Water* 3, 327–368
66. Australian Centre for International Agricultural Research (2014) *Crop Yields and Global Food Security*, Australian Centre for International Agricultural Research
67. Wu, A. *et al.* (2016) Connecting biochemical photosynthesis models with crop models to support crop improvement. *Front. Plant Sci.* 7, 1–16
68. Wu, A. *et al.* (2018) Simulating daily field crop canopy photosynthesis: an integrated software package. *Funct. Plant Biol.* 45, 362–377
69. Wright, I.J. *et al.* (2004) The worldwide leaf economics spectrum. *Nature* 428, 821–827
70. John, G.P. *et al.* (2017) The anatomical and compositional basis of leaf mass per area. *Ecol. Lett.* 20, 412–425
71. John, G.P. *et al.* (2013) Allometry of cells and tissues within leaves. *Am. J. Bot.* 100, 1936–1948
72. Pickard, W.F. (1982) Why is the substomatal chamber as large as it is? *Plant Physiol.* 69, 971–974
73. Lichtenberg, M. *et al.* (2017) Light sheet microscopy imaging of light absorption and photosynthesis distribution in plant tissue. *Plant Physiol.* 175, 721–733
74. Verboven, P. *et al.* (2015) Synchrotron X-ray computed laminography of the 3D anatomy of tomato leaves. *Plant J.* 81, 169–182
75. Kittelmann, M. *et al.* (2016) Serial block face scanning electron microscopy and the reconstruction of plant cell membrane systems. *J. Microsc.* 2, 200–211